First online: 20 April 2017

Numerical Versus Simplified Analytical Approach for Prediction of Flexural Strength in LG Beams

Giuseppe Campione[1], Francesco Parrinello[2]

[1,2]Department of Civil, Environmental, Aerospatiale and Materials (DICAM), University of Palermo, Viale delle Scienze, 90128 Palermo, Italy

[1]giuseppe.campione@unipa.it

***Abstract*-Flexural behavior of laminated glass beams was numerically predicted through an open source finite element code; a cohesive-frictional behaviour of the adhesive and the brittle fracture of the glass were implemented though adequate constitutive laws. Both the processes of de-bonding of interlayer and the failure of glass panels can be captured by a refined finite element analysis. Based on the elastic theory, simple analytical expressions are utilized for the prediction of composite glass beams, including the extreme cases of full composite and layered behaviour. Cases of study refer to glass composite beams having T or I cross-section shapes. Beams consist of laminated glass (LG) flanges and LG web that is assembled together by different kinds of polymer adhesive (semi-rigid i.e., silicones, modified silicones and polyurethanes and rigid i.e., epoxy resins, acrylics). Experimental data given in the literature was utilized to show the effectiveness of numerical model to reproduce experimental results, and to show the effectiveness of the proposed elastic model for preliminary beams in flexure design.**

Keywords- Glasses; Adhesion; Mechanical Testing; Assembly

I. INTRODUCTION

It is only during the last few decades that glass application has evolved from purely decorative to structural; in the past it was used as a construction material. Together with good mechanical properties, the qualities of transparency and translucency have allowed innovative glazing structures in contemporary architecture, in which laminated glass is used more frequently. In this field, it is well known that assembling thin laminated glass panels makes glass members. Every panel is constructed by coupling two or more glass foils, connected by means of an interlayer. In most cases, annealed float glass is used because of its better post breakage behaviour, as well as lower costs when compared to fully tempered glass, which is more expensive and fails in many small fragments. The interlayer has viscous-elastic behaviour, normally formed by a polyvinyl butyral (PVB), polycarbonate (PC), or ethylene-vinyl acetate (EVA) film. It is well known that structural glass members are made by assembling thin laminated panels, which can be connected with different bonding techniques, such as steel devices or with structural adhesives. The latter are very commonly used because they do not reduce the transparency of the member, and because of the holes, stress concentrations are avoidable. This technique is used to make up columns in glazing structures. Different applications of the technique can be found in contemporary architecture. As evidenced by the literature, buckling phenomena, which results from the slenderness of the panels, causes one of the most important problems in such members.

An important aspect for the design of glass beams is the shape and size choices of the transverse cross-section, which can provide good performance in terms of both resistance and deformation capacity (ultimate and serviability limit states). These states correspond to the reaching of the tensile strength of the glass, debonding of glue adhesive, critical load due to lateral buckling phenomenon, and maximum allowable deflection. The closed shape (circular or rectangular hollow) is the best structural shape for the cross-sections, but its use makes it difficult to maintain the transparency of the element. The shapes most used are therefore open sections such as T and I shapes (see Fig. 1). The literature [1] gives examples of using these shapes. Comparing glass beams having rectangular cross-section (with t thickness almost 1/10 of the height h) loaded along the weakest plane or the plane of maximum inertia shows that the strength ratio (ratio between the resistant modules) is 10 and the deformability ratio (ratio of the moments of inertia) is 100. Therefore, members with rectangular cross-sections loaded along the weakest plane are conditioned in the design by the deformability limits. By contrast, if loaded along the maximum inertia, they are conditioned by the strength limits (glass in tension). Flexural strength is limited by torsional stiffness of open cross-section if slender cross-sections are utilized, which is negligible. Therefore exceeding the rectangular limit of L/h= 20, 35 and 50 (L is the length of the beam and h the height of the cross-section), T or I cross-sections flexural buckling phenomenon drastically reduces the flexural capacity. Each rectangular glass panels forming open cross-sections with T or I shapes is generally a laminated glass (LG) panel, each constituted by two or more glass sheets that are connected with a flexible interlayer (e.g. PVB). The knowledge of the interlayer mechanical properties, which is a function of temperature and load duration, allows one to evaluate the mechanical behaviour of the composite glass [2-8] which is defined between the two limit behaviours, respectively corresponding to the monolithic beam and the layered case.

DOI: 10.5963/JCES0601001

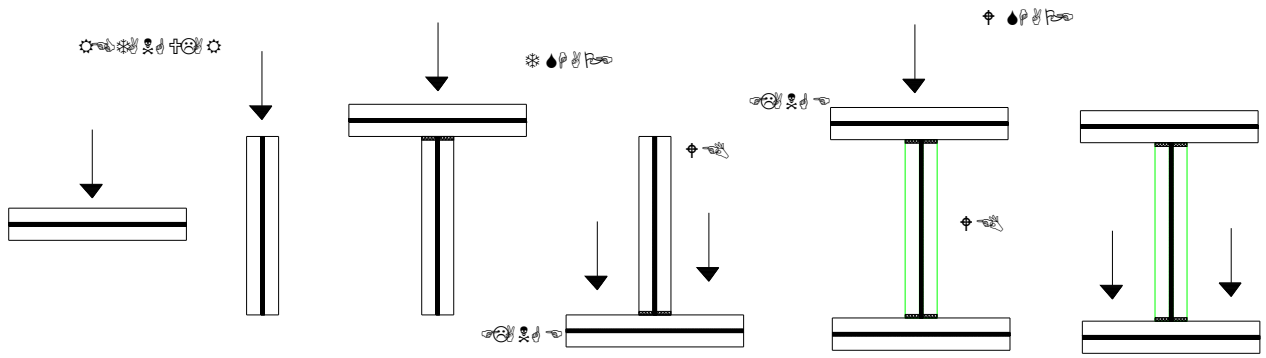

Fig. 1 T and W cross-sections fabricated from LG plates assembled with glue adhesive

It is necessary to utilize a strong and stiff adhesive layer for connection of single glass sheets and/or LG panels in order to ensure monolithic structural behaviour of open cross-section (T or W shape). The adhesive should provide good resistance to static loads, to fatigue and shock, while maintaining transparency of the composite elements. In contrast, glass composite elements are more sensitive to temperature variation and long-term loading conditions due to the presence of viscous phenomena at the interlayer [1] Shear resistance and shear modulus of adhesive are important characteristics and have a major influence on the glass beams' load-carrying capacity and structural behaviour [2]. The stiffness of the bonded connection depends on the shear stiffness of the adhesive (shear modulus with time-dependent effects) and the geometry of the joint (depth, thickness). Increasing thickness of the adhesive will decrease the stiffness of the joint. Enlargement of the joint width leads to an increase in stiffness of the whole connection. Therefore, because of the small bonding area, direct connections on the face of the glass sheets have low stiffness (see Fig. 2).

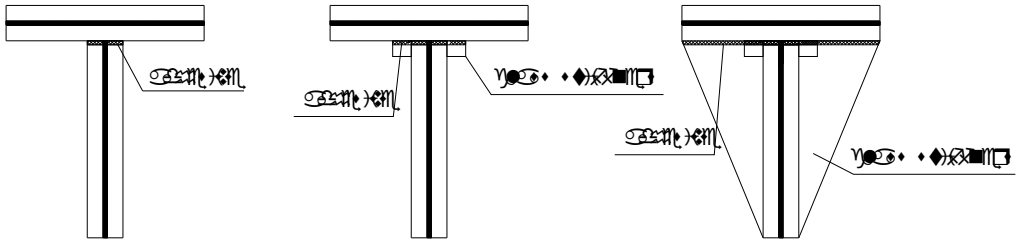

Fig. 2 Gluing technique for T glass beams

Strength and stiffness are the primary requirements of the adhesive layer. Common adhesives can be divided according to their modulus of elasticity and shear modulus into flexible-elastic (i.e., silicones, modified silicones, and polyurethanes) and rigid (i.e., epoxy resins, acrylics). In comparison with elastic adhesives, stiff adhesives offer extremely high strength, but very low elongation, which shows elongation at failure even exceeding 250%. Practical application of different types of polymer adhesives depends on their behaviour under loading. During the selection, special emphasis has to be devoted to the UV (ultraviolet) stability and long-time behaviour of the chosen adhesives. The maximum strength of the adhesive depends on several factors, such as thickness and type, with values ranging from 0.5 to 10 MPa. Tests carried out by [9] provided the adhesive shear strength values. They vary with the thickness (1, 2, and 3 mm) and with the type (acrylic, polyurethane, silicone) of adhesive. For silicone, polyurethane, epoxy, 2P-acrylic and UV-acrylic, [10] gave mean shear strength values (based on short-term loading and equivalent constant shear stress along 26 mm long) equal to 0.58, 0.97, 7.21, 15.30, and 9.83 MPa. Finally, a heat transfer analysis and its thermal properties must be considered in the prediction of flexural strength beams. Despite it being out of the scope of this paper, because the dilatation coefficient is very important in the elongation factor of the polymer adhesives, they are of interest for community researcher and have to be included in a more complete model.

II. NUMERICAL ANALYSIS

At the moment, nonlinear analyses are one of the best ways to accurately predict the experimental response of LG beams for the reason that they allow one to include fracture mechanics for glass members, and nonlinear behaviour of the PVB interlayer and adhesive [3-12]. The numerical analyses performed here utilized a simplified modelling technique. It consisted of discretizing the glass beams with elastic material out of the loaded and supported sections, where zero thickness interface

DOI: 10.5963/JCES0601001

elements with elastic-brittle behaviour, were introduced in order to simulate the fracture process on four fixed positions (see Fig. 3). Time-dependent effects are not included in the model. In order to take these effects into account, the effective thickness of LG panels can be utilized as suggested in the literature [13]. Time-dependent effects on the adhesive are also important aspects to take into account, however, they are not an object of current research. A study of the time-dependent effects of the glued connection can be found in the literature [10]. The constitutive parameter of such interface elements produces the same fracture energy as the glass. The glues were modelled with cohesive frictional constitutive laws and zero thickness interface elements. Utilized in open source FEAP code) [14], the mesh, constituted by shell elements was defined with six blocks of nine-node elements for the glass panels, divided into 4 elements in the vertical direction, and 40 elements in the horizontal direction. The blocks of glass material were defined by the Young's modulus and the Poisson ratio and constitutively modelled as elastic and isotropic. A material with elastic-brittle behaviour whose parameters are described below defined the vertical glass interface, while the adhesive was modelled as a horizontal interface of zero thickness and frictional cohesive bond whose constitutive parameters are described below (see Fig. 3).

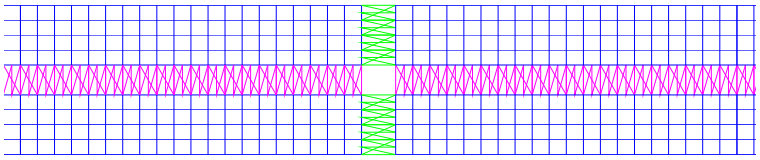

Fig. 3 Horizontal and vertical interfaces adopted in FEM analyses

The interlayers' mechanical behavior is quite complex, including several phenomena such as de-cohesion, viscosity, frictional effects, and more. In the present paper, due to viscosity, the long-term effects, are neglected and the mechanical behaviour of the gluing layer is modelled in the damage theory framework, considering progressive debonding, in which the evolution of the damage parameter decreases with the ability to maintain the two joined glass panels. This model was implemented in an open source finite element code, for a zero thickness interface element, and with the constitutive law shown in Fig. 4.

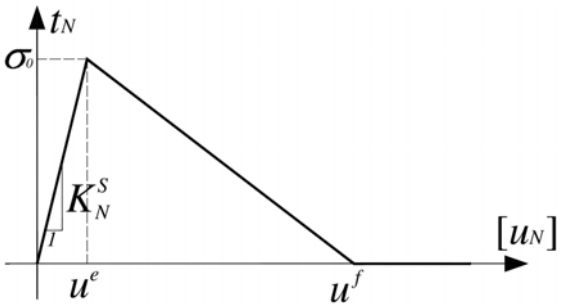

Fig. 4 Mode I interface numerical response

Due to the symmetry condition with respect to the central vertical axis, only half of the specimen was discretized into finite elements and the relevant boundary condition was introduced on the left side (see Fig. 5).

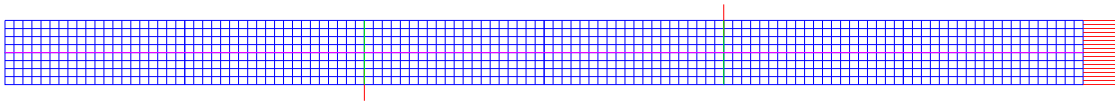

Fig. 5 Complete FEM model in FEAP code

From the kinematical point of view, the interface deformation state is modelled by the displacement discontinuity between the connected bodies' edges. As shown by Fig. 6, this relative displacement is expressed as $[u]=u^+-u^-$, where u^+ and u^- are displacement vectors on the positive and negative sides. Displacement jump $[u]$ can be represented by the normal component u_N (Mode I) and the tangential component u_T (Mode II). In order to introduce the damage variable, let us consider the representative surface element (RSE) plotted in Fig. 6, where ΔS is the area of RSE, ΔS measures the area the sound fraction of RSE, and ΔS_C measures the area of the RSE cracked fraction.

The damage variable is defined as:

DOI: 10.5963/JCES0601001

$$\omega = \frac{\lim}{\Delta S \to 0} \frac{\Delta S_C}{\Delta S}. \tag{1}$$

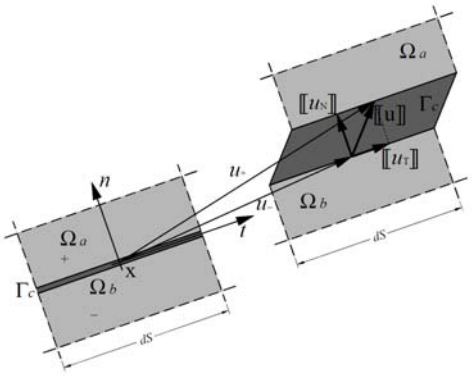

Fig. 6 Interface displacement model

As shown in Fig. 7, the areal density of micro-cracks in an infinitesimal RSE is measured by the damage variable ω. It can be also identify the extension of the cracked fraction as $(1-\omega)dS$ and similarly, the extension of the sound fraction as ωdS. It is also possible to adopt a specific constitutive law for each fraction. For example, a linear elastic law for the uncracked fraction and an elastic-plastic law for the cracked fraction. In other words, the model assumes the damage variable ω as a discriminant that governs the evolution and the transition of the interface behaviour from the initial elastic regime of the sound interface to the residual frictional behaviour of the completely delaminated one (Fig. 7).

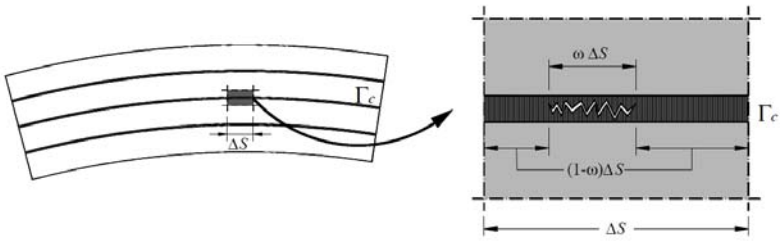

Fig. 7 RSE fractions at mesoscale

As shown in Fig. 8, the two fractions produce two distinct distributions of traction τ_S and τ_C from the static point of view.

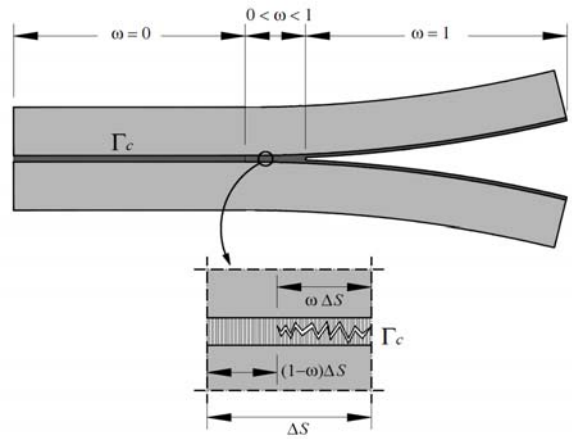

Fig. 8 Fraction identification through damage parameter ω

Following a classical homogenization procedure, the RSE average traction can be defined as

DOI: 10.5963/JCES0601001

$$t_S = \lim_{\Delta S \to 0} \frac{1}{\Delta S} \int_{\Delta s} \tau_s dS \tag{2}$$

$$t_c = \lim_{\Delta S \to 0} \frac{1}{\Delta S} \int_{\Delta s} \tau_C dS \tag{3}$$

which are two traction vectors acting on the same infinitesimal area dS (Fig. 9).

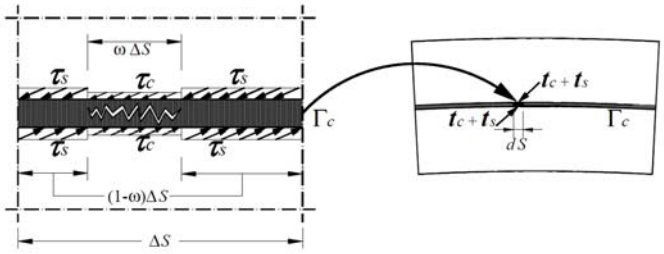

Fig. 9 Stress distribution and superposition of traction vector t

The total traction is then

$$t = t_S + t_c \tag{4}$$

The two distinct constitutive laws of the fractions allow us to write tractions in Eqs. (4, 5) in the following form

$$t_S = \omega K_S \delta_S^e \tag{5}$$

$$t_C = (1-\omega) K_C \delta_C^e \tag{6}$$

where

$\delta_S^e = [u] - \delta_S^p$ is the elastic deformation of the integer fraction and δ_S^p the plastic component;

$\delta_C^e = [u] - \delta_C^p$ is the elastic deformation of asperities in the cracked fraction and δ_C^p is the relevant plastic component due to asperities relative to the parts in contact (see Fig. 10a, b, c).

Fig. 10 Asperities deformation components

The adopted constitutive model ensures that the entire process is thermodynamically consistent, and that the energy dissipation is always positive (for details [10]). Damage evolution is managed by the following damage activation law and relevant flow rules

$$\phi_d = Y - Y_0 - \chi(\xi) \le 0 \tag{7}$$

$$\dot{\omega} = \frac{\partial \phi_d}{\partial Y} \dot{\lambda} \quad \dot{\xi} = \frac{\partial \phi_d}{\partial \chi} \dot{\lambda} \tag{8}$$

where

$Y = \frac{1}{2} u_S^T k_s u_S - \frac{1}{2} u_C^T k_C u_C$ is the strain energy release rate, $\chi(\xi)$ is the softening variable, and Y_0 is a threshold value.

DOI: 10.5963/JCES0601001

Plastic deformations are neglected in the sound fraction $\left(\delta_S^p = 0\right)$, whereas in the cracked fraction, a classical non-associative Mohr-Coulomb law, which allows one to assume a dilatancy angle independent of the friction angle, models the evolution of plastic deformations. Using Eqs. (6, 7, 8), it can be obtained:

$$t = \omega K_S \delta_S^e + (1-\omega) K_C \delta_C^e \tag{9}$$

The adopted constitutive law produces the pure Mode I response in terms of stress vs. strain, where σ_O is the maximum stress, k_N^S is the elastic stiffness, and u^f is the ultimate displacement jump, which produces the following fracture energy:

$$G_I = G_{II} = \frac{1}{2}\sigma_o u^f = \frac{1}{2} k_N^S u^e u^f . \tag{10}$$

For elastic glass, the constitutive parameters are: Young's modulus E = 70 GPa and Poisson's ratio ν = 0.23, which are consistent with the standard [13].

Moreover, as suggested in standard [13], for vertical interfaces constituting the fracture zones of the glass toughness $k_I = 0.75 \frac{MPa}{m}$ and a tensile strength of 42 MPa were assumed. Therefore, the fracture energy is defined as:

$$G_I = \frac{k_I^2}{E} = \frac{0.75^2}{70000} = 0.080357 \frac{N}{mm} . \tag{11}$$

By taking into account the relationship between fracture energy and ultimate displacement in Eq. (12) the ultimate displacement is:

$$u^f = \frac{2G_I}{k_N^S} = 0.0038265 mm \tag{12}$$

The interface elastic stiffness k_N^S is calculated considering an ultimate elastic displacement assumed as:

$$u^e = \frac{u^f}{2} = 0.0019132 mm \tag{13}$$

and therefore

$$k_N^S = \frac{\sigma_0}{u^e} = 219521.7 \frac{N}{mm^3} \tag{14}$$

In agreement with the values suggested in [13] in the case of stiff and strong adhesive (type 1), it was assumed the Young elastic modulus E = 2.500 N/mm^2, Poisson ratio ν = 0.45, tangential elastic modulus G = 862.07 N/mm^2, and tangential strength τ0=12 MPa. Once the shear modulus is known, the shear elastic deformation γe is calculated as:

$$\gamma_e = \frac{\tau_0}{G} = 0.01392 \tag{15}$$

and the [13] derive the value of the ultimate shear strain as $\gamma_f = 0.2$, making it possible to calculate the interface constitutive parameters u_e and u_f by multiplying the shear strength by the adhesive thickness h=0.38 mm

$$u^e = \gamma_e h = 5.189 \cdot 10^{-3} mm \tag{16}$$

$$u^f = \gamma_f h = 0.076 mm \tag{17}$$

Finally, the interface tangential elastic stiffness is

DOI: 10.5963/JCES0601001

$$k_T^S = \frac{\tau_0}{u^e} = 2268.6 \frac{N}{mm^3} \tag{18}$$

In the case of flexible and low strength adhesive (type 2), the strength, fracture energy, and constitutive parameters were chosen after some numerical analyses. In this way, it was possible to reproduce an adhesive with a lower fracture energy than the previous one, such that the breaking of the glass occured after debonding during the loading phase. The assumed parameters are: $k_T^S = k_N^S = 2268.6 \frac{N}{mm^3}$, $u^e = 0.000132mm$, $u^f = 0.038mm$ and shear strength 0.85 MPa. To show the effectiveness of the proposed model, a numerical example was created.

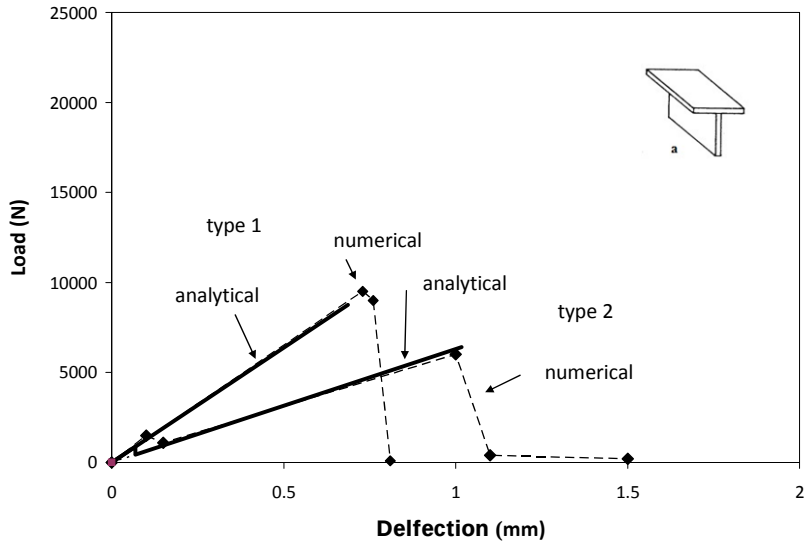

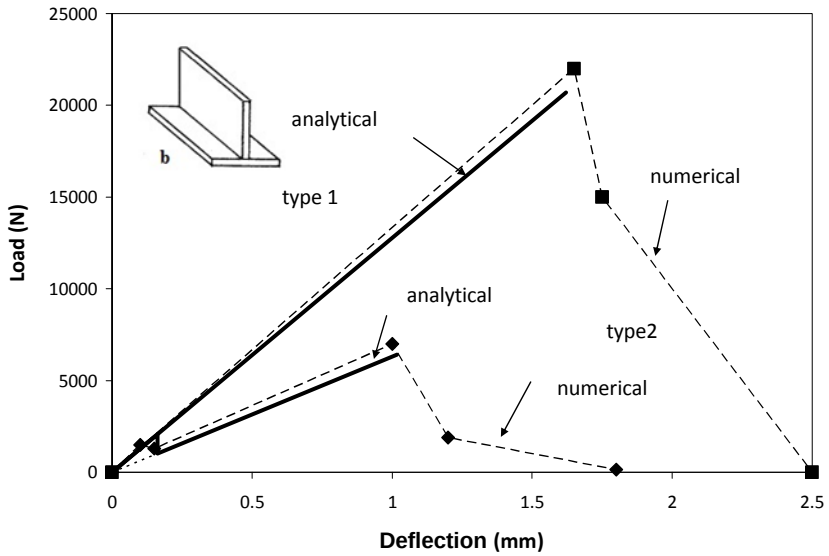

DOI: 10.5963/JCES0601001

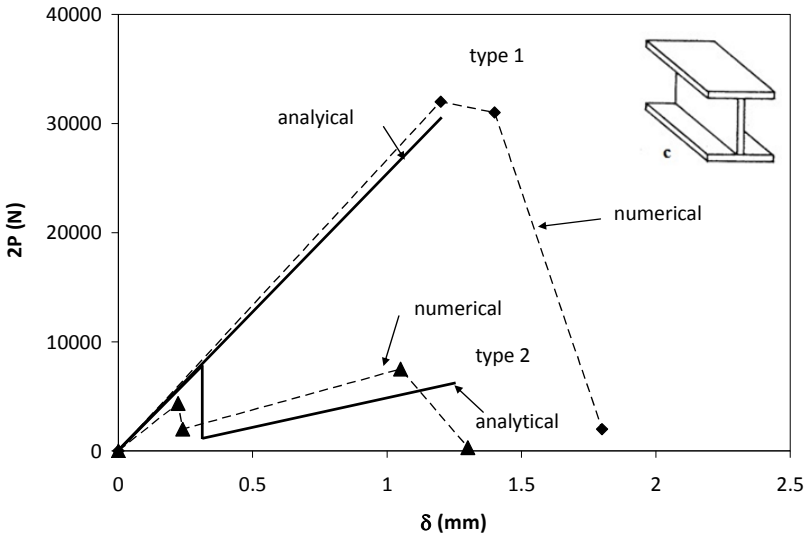

Fig. 11 Numerical versus analytical load-deflection curves for T and W LG beams

The case examined refers to glass beams having span 1000 mm tested in four-point bending tests. Both with a 10 mm (4+0.38+4) thickness, the sections examined were T and W shapes having flanges 100 mm and web 120 mm. LG had tensile strength of 42 MPa. The cases examined refer to high and low strength glue, and with 2 MPa and 0.85 MPa shear strength, respectively. In the same graph, the analytical results obtained with the simplified analytical model are also described and shown below.

The comparison shown in Fig. 11 for T beams with a flange on the top (Fig. 11a), on the bottom (Fig. 11b), and a W shape (Fig. 11c) stressed that if the adhesive resistance is low (0.85 MPa), there are no significant differences between the use of a T or W cross-section. It also stressed that the strength and stiffness of the open cross-section is almost identical to the web section, the W shape behaves better than the T shape if more resistant adhesive (2 MPa) is utilized, and the T shape with a flange on the bottom has a better load-carrying capacity compared to T beams with a flange on the top.

The glass beams were brittle in all of the examined cases. This aspect has to be considered in adopting an adequate safety factor for the design of glass beams, which should be higher than the material factor in the opinion of the authors for the reason that it depends on the glue characteristics of the glass surface, as well as the geometrical characteristics of the adhesive. To draw more general conclusions, more experimental researches based on real-scale experiments and on refined theoretical analysed are required.

III. SIMPLIFIED APPROACH

Fig. 12 shows the simplified analytical model to predict the load-deflection response of composite glass beams in flexure. According to this model the response of the beam is between the response of connected and unconnected beams.

Specifically, in the first phase, the response of the beam follows the behavior of the connected beam up to P_d. Due to shear failure, the external load drops to P_{dr}, occurring at the same load level as the unconnected beam. From simple geometrical considerations the displacements corresponding to Pdr can be obtained as:

$$\delta_d = \left(\frac{\delta_{uc}}{\delta_{ud}} \right) \cdot P_d \tag{19}$$

$$P_{dr} = \left(\frac{\delta_d}{\delta_{ud}} \right) \cdot P_d \tag{20}$$

δuc and δud being the deflections of the connected and unconnected beams at flexural failure.

Given below are the expressions of maximum deflection in the elastic range of simply supported glass beams.

DOI: 10.5963/JCES0601001

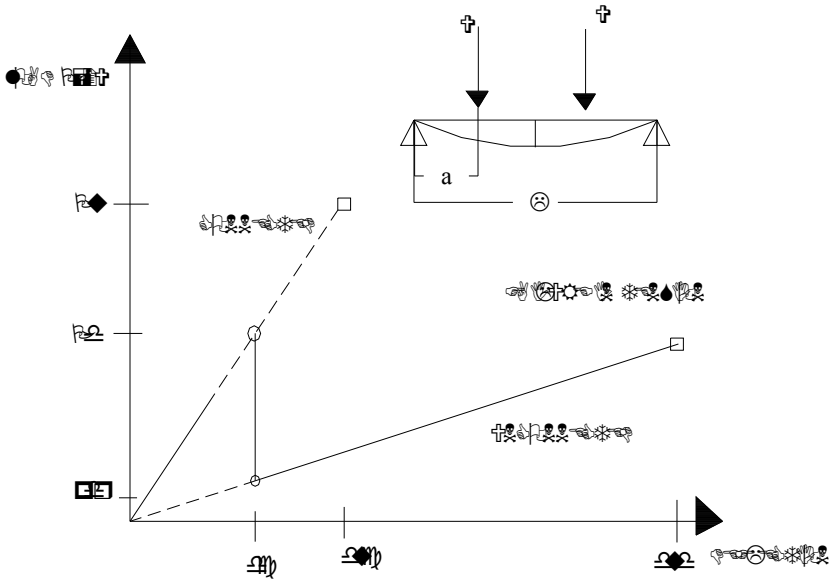

Fig. 12 Simplified load-deflection responses of LG composite beams

In the four-point bending tests the deflection proves to be the following:

$$\delta_{\max} = \frac{P \cdot a^2}{2 \cdot E \cdot J} \cdot \left(L - \frac{4}{3} \cdot a \right) \tag{21}$$

P being the external load and the shear span.

The maximum shear stress at the fiber between flange and web is expressed by the Jourasky formula:

$$\tau = \frac{P}{2 \cdot J \cdot t} \cdot b \cdot t \cdot \left(a - \frac{h}{2} \right) \tag{22}$$

If τ assumes the value lim, Eq. (22) gives the Pd expressed as:

$$P_d = \frac{\tau_{\lim}}{b \cdot d \cdot \left(a - \frac{d}{2} \right)} \cdot J \cdot c \tag{23}$$

With J the moment of inertia of open cross-section.

As observed in Overend and Watson (2011), the value of τlim depends on the type of glue, the glass surface, and the thickness and width of the glued section.

The ultimate load P_{ud} (corresponding to δ_{ud}) is derived as $P_{ud} = \frac{W \cdot f_{ct}}{a}$, with W indicating the elastic modulus of cross-section, assuming the lower and the upper values for full connection, absence of connection, and f_{ct} the tensile strength of LG panels.

IV. VALIDATION OF PROPOSED MODEL

The recent experimental investigations by the author were considered [15-17] (to validate the analytical and the numerical model proposed here. Unfortunately, because none were available in the literature in a complete form, it was not possible to add any other experimental investigation on the flexural behaviour of beams with T or I cross-section shapes (Ply, 1988). Also, because of the absence of specific experimental data, no ad-hoc specific validation of the adhesive for connection of T or W shape glass beams is made. The first case examined shown in Fig. 13 refers to the experimental research by Campione et al. (2013), in which twelve specimens were prepared and tested under a four-point bending apparatus. Six specimens were

DOI: 10.5963/JCES0601001

monolithic, six were laminated, and the two sets of specimens came from two different manufacturers. Six of them were type 1 with tensile strength 36 MPa and six were type 2 with tensile strength 42 MPa. All beams had a width of 100 mm and a length of 300 mm. The layered glass beams were obtained from individual glass panels of 4 mm thickness, assembled with PVB with nominal 1 mm thickness. According to the manufacturer, 8.38 (4+0.38+4) was the effective thickness of the layered panels.

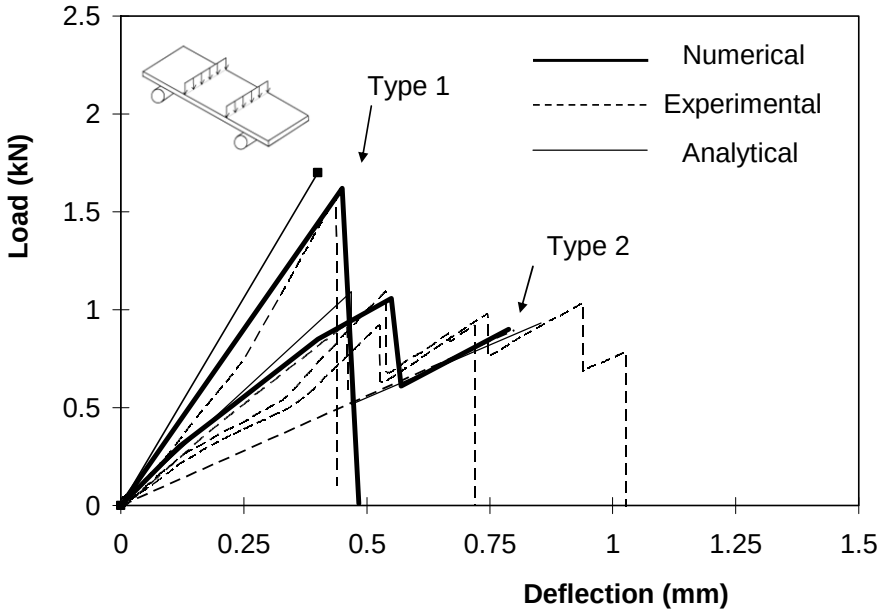

Fig. 13 Load-deflection curves for layered glass beams tested in [15]

Fig. 13 shows the load-displacement diagrams relative to the four-point bending tests on the two series of LG beams. With brittle-type fracture and a simultaneous crisis for both plates, type 1 presented very similar behaviour to monolithic glass panels. Fig. 13 shows the numerical and the experimental responses (average curves) for the layered beams.

For type 1, the failure load obtained numerically (1620 N) almost coincided with the experimental value (1570 N), while the stiffness, and consequently the ultimate displacements were slightly different. The deflection obtained in the numerical analysis was 0.45 mm, while the relevant experimental value was 0.43 mm. For maximum load and corresponding deflection, the values derived from the theory of elasticity were 1720 N and 0.39 mm, and both values were close to the numerical ones. Without debonding of the two glass sheets, the numerical simulation reproduced monolithic behaviour up to rupture for layered beams. The analytical model also gave an accurate prediction of the experimental results (especially failure modes and peak loads). For type 2 glass beams, the maximum load of 975 N was reached for the numerical analysis and 1058 N for the experimental one, while the deflections were 0.50 mm and 0.55 mm. The most important aspect of the latter analysis is definitely the good reproduction of the behaviour in the softening branch. Indeed, it gradually damaged during the loading phase up to complete debonding, while the plates were mechanically uncoupled and were still in the elastic regime. From the numerical analyses, it is clear that the main mechanism governing the structural behaviour was debonding.

The second examined case refers to the experimental research by [15], in which twenty specimens were prepared and tested under a four-point bending apparatus. One series of beams had a height of 125 mm and a thickness of 20 mm (9+9+0.78). Another series had a height of 500 mm and a thickness of 20 mm (9+9+0.78). The span was 850 mm. To avoid buckling effects, special supports and steel clamps were utilized in the loaded section. Beams were loaded along the plane of maximum inertia. Fig. 14 shows the load-displacement diagrams relative to the four-point bending tests on the two series of glass beams. Almost monolithic behaviour was observed experimentally both for medium-scale (125x20) and large-scale (500x20) beams. Analytical prediction gave accurate results in terms of peak load or small-scale specimens, while large-scale beams underestimated the peak load in the range of 15%. The best prediction of the experimental results is given by the numerical results, including the softening ranges.

DOI: 10.5963/JCES0601001

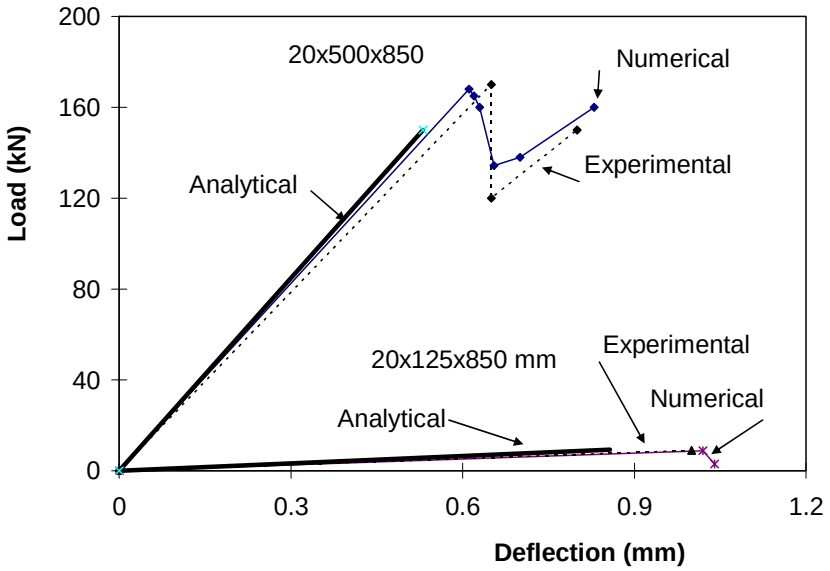

Fig. 14 Load-deflection curves for layered glass beams tested in [16]

Third cases examined refers to the experimental research of [17], in which three-point bending tests are presented on laminated glass specimens, made with an internal float glass, and two external equal tempered glass panels. Three different combinations of annealed float characterized the laminated glass specimens, of equal cross section, and fully thermally tempered glass piles. In addition, two sets of specimens were constructed, with two different interlayers having significantly different mechanical properties. The flexural load was applied parallel to the lamination plane (in-plane loading) and the tests were conducted at room temperature. The specimens, three for both float and tempered glass layers, showed a linear load–deflection response until brittle fracture occurred at an average strength of fct1=45 MPa and fct2=130 MPa, respectively. The height of the beams was h=150 mm and the span L= 1350 mm. LG beams where constituted by three glasses; two external tempered glass and one internal float glass having external thickness of each layer t1 and thickness of internal layer t2. 30 mm (12-6-12, 10-10-10, 6-18-6) was the whole thickness of the beams. Two different interlayer (PVB and SPG) were utilized. As stressed by [17] the interlayer plays a significant role in defining the flexural response of in-plane loaded, layered beams, and the progressive failure detected for the laminated glass/SGP beams is significantly different than what has been noted for the laminated glass/PVB beams. Consequently, the quality of the used interlayer affects the post cracking range. By adopting the current model, it was only possible to examine the effect of the different strength of single glasses, and not the influence of the type of interlayer. As shown in Fig. 15, the results in the case of using PVB interlayer were satisfactory.

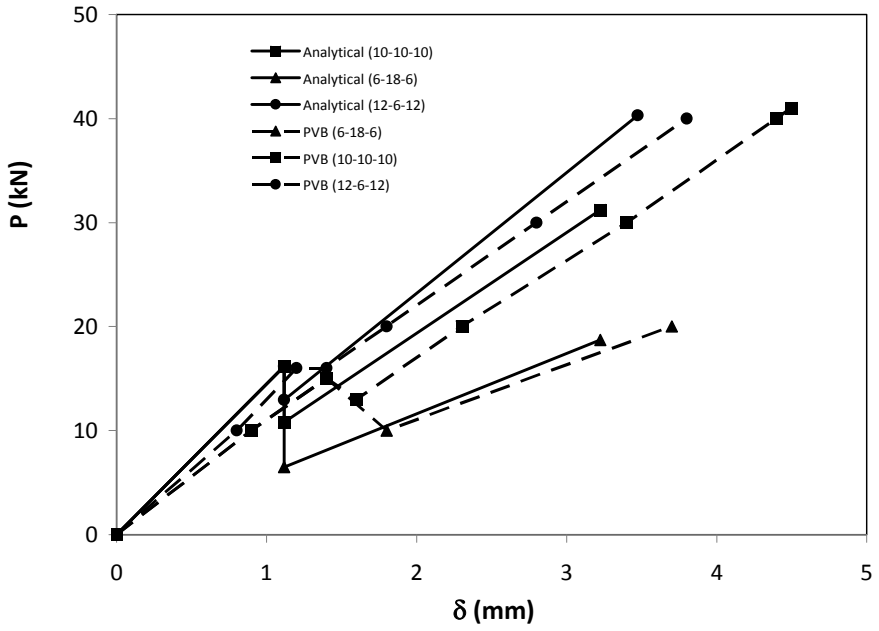

Fig. 15 Load-deflection curves for layered glass beams tested in [17]

DOI: 10.5963/JCES0601001

Fig. 15 shows the load-displacement diagrams relative to the third points bending tests on glass beams. Monolithic behaviour was observed experimentally for both medium (125x20) and large scale (500x20) beams. In the analytical prediction the deflection of the beams at first cracking and at failure were determined with the expression $\delta_{\max} = \frac{P \cdot L^3}{48 \cdot E \cdot J}$. Adopting at first cracking (P=P1) $J_1 = \frac{1}{12} \cdot t \cdot h^3$ and $P_1 = \frac{2}{L} \cdot \frac{t \cdot h^2}{6} \cdot f_{ct1}$ and at failure (P=P2) $J_1 = \frac{1}{12} \cdot 2 \cdot t_1 \cdot h^3$ and $P_1 = \frac{2}{L} \cdot \frac{2 \cdot t_1 \cdot h^2}{6} \cdot f_{ct2}$.

V. CONCLUSIONS

A simplified analytical model based on elastic theory, a numerical nonlinear analysis based on fracture mechanics, and the use of cohesive model for interlayer and adhesive connections was utilized to examine the flexural behaviour of laminated glass beams.

The focus was on the flexural behaviour of glass composite beams having T or W shapes of the transverse cross-section.

The results obtained showed that if flexible and low-strength adhesive is utilized (e.g. silicone), there is no significant difference between the use of a T or W cross-section and the flexural strength of glass beams is that of the web section; if rigid and high-strength adhesive is utilized (e.g. acrylic) the W shape behaves better than the T shape; and compared to T beams with a flange on the top, the T shape with a flange on the bottom has a better load-carrying capacity.

The simplified elastic model gives results in good agreement with experimental and numerical results available in the literature and proves to be a useful instrument for preliminary design of glass beams.

In future research, time-dependent effects on adhesive are important aspects to take into account. Also, because of the absence of specific experimental data, no ad-hoc specific validation of the adhesive for connection of T or W shape glass beams was created. Further experimental activity specifically designed to study the efficiency of adhesive would be helpful for the whole scientific community.

REFERENCES

[1] A. Pye and S. Ledbetter, "The selection of an adhesive for the construction of a glass-adhesive T-beam," *Int. J Adhesion and Adhesives*, vol. 118, pp. 159-165, 1998.

[2] R. A. Behr, J. E. Minor, M. P. Linden, and C. V. G. Vallabhan, "Laminated glass units under uniform lateral pressure," *ASCE J of Structural Engineering*, vol. 111(5), pp. 1037-1050, 1985.

[3] C. V. G. Vallabhan and B. Y.-T. Wang, "Nonlinear analysis of rectangular glass by finite difference method," Institute for Disaster Research, Texas Technical University, Lubbock, TX, June 1981.

[4] S. J. Bennison, C. A. Smith, and A. Van Duser, "Structural performance of laminated glass made with a stiff interlayer," *Symp. on the Use of Glass in Buildings*, Pittsburgh, 9 pages, 2002.

[5] S. Briccoli Bati, G. Ranocchiai, C. Reale, and L. Rovero, "Time-dependent behavior of laminated glass," *ASCE J Mat in Civ Eng*, vol. 22(4), pp. 389-396, 2010.

[6] L. Galuppi and G. F. Royer-Carfagni, "Effective thickness of laminated glass beams: New expression via a variational approach," *Engineering Structures*, vol. 38(4), pp. 53-67, 2012.

[7] R. A. Behr, J. E. Minor, M. P. Linden, and C. V. G. Vallabhan, "Laminated glass units under uniform lateral pressure," *ASCE J of Structural Engineering*, vol. 111(5), pp. 1037-1050, 1985.

[8] M. Overend, Q. Jin, and J. Watson, "The selection and performance of adhesive for a steel-glass connection," *International Journal of Adhesion & Adhesive*, vol. 31(7), pp. 587-597, 2011.

[9] M. Netusil and M. Eliasova, "Design of the composite steel-glass beams with semi-rigid polymer adhesive joint," *Journal of Civil Engineering and Architecture*, vol. 6(8), pp. 1059-1069, 2012.

[10] R. A. Behr, J. E. Minor, and M. P. Linden, "Load duration and interlayer thickness effects on laminated glass," *J Struct Eng, ASCE*, vol. 112(6), pp. 1441-1453, 1986.

[11] A.K.W. So and S.L. Chan, "Nonlinear finite element analysis of glass panels," *Journal of Engineering Structures*, vol. 18(8), pp. 645-652, 1996.

[12] M. Fröling and K. Persson, "Computational methods for laminated glass," *J. Eng. Mech.*, vol. 139(7), pp. 780-790, 2013.

[13] CNR DT 210/2012, "Consiglio Nazionale delle Ricerche, Istruzioni per la Progettazione, l'Esecuzione ed il Controllo di Costruzioni con Elementi Strutturali di Vetro," Roma, 2012.

[14] R.L. Taylor, "FEAP - A Finite Element Analysis Program, Version 7.5 User Manual," *Department of Civil and Environmental Engineering*, University of California at Berkeley, 2005.

DOI: 10.5963/JCES0601001

[15] G. Campione, S. Colaianni, and G. Minafò, "The use of steel angles for the connection of laminated glass beams: experimental and modelling," *Construction and Building Materials*, vol. 29(4), pp. 682-689, 2012.

[16] G. Campione, M. Di Paola, and G. Minafò, "Laminated glass members in compression: experiments and modelling," *ASCE Journal of Structural Engineering*, vol. 138(2), pp. 234-245, 2013.

[17] L. Biolzi, S. Cattaneo, and G. Rosati, "Progressive damage and fracture of laminated glass beams," *Construction and Building Materials*, vol. 24(4), pp. 577-584, 2010.

DOI: 10.5963/JCES0601001